Radiation guided along a cylindrical symmetry system according to the refractive index profile

C. Alejandro Paola
Facultad de Ciencias Astronómicas y Geofísicas, Univesidad Nacional de La Plata,
Paseo del Bosque s/n, La Plata, Buenos Aires, Argentina;
TE: (54) 221 4236593. Fax: (54) 221 4236591.
Universidad Tecnológica Nacional, Facultad Regional La Plata,
Avenida 60 esquina 124 s/n, La Plata, Buenos Aires, Argentina;
Tel: (54) 221 4124300,
e-mail: apaola@fcaglp.unlp.edu.ar

A. Cruzado
Facultad de Ciencias Astronómicas y Geofísicas, Univesidad Nacional de La Plata,
Paseo del Bosque s/n, La Plata, Buenos Aires, Argentina;
TE: (54) 221 4236593. Fax: (54) 221 4236591.
Instituto de Astrofísica de La Plata, CONICET,
Paseo del Bosque s/n, 1900 La Plata, Buenos Aires, Argentina,
e-mail: acruzado@fcaglp.unlp.edu.ar; alicehaiadjamian@yahoo.com.ar

Received 3 January 2020; accepted 25 August 2020

We aim at finding, from purely theoretical analysis, the behavior that the refractive index should have within a cylindrical waveguide so that the radiation entering the system in a definite way is guided through it. Based on the criterion we have set in a previous article applying the Fermat's extremal principle, in the framework of the geometrical optics, we depict the radiation confinement regions for refractive index profiles often used in the construction of waveguides, one step, multi-step and parabolic, by drawing upon the Legendre transform space as an intermediate resource in the process. We have also studied the possibility of performing the reverse path: for a wanted confinement region, to find the parameters defining the refractive index profile of the waveguide to be built. We conclude that such a process is possible as long as we know the shape of the profile. Under such restriction, our analysis allows us to deduce the characteristics that the guide should have so that the radiation entering with a given angle and at a certain distance from its axis remains confined. The technique can be used in design processes as a resource to limit the parameters that characterize the system.

Keywords: Optics; geometric optics; waveguides; technical applications.

PACS: 42.00.00; 42.79.e.

DOI: https://doi.org/10.31349/RevMexFis.66.803

1. Introduction

The confinement and guidance of electromagnetic radiation in dispersive media due to total internal reflection is of great interest in many fields of theoretical physics, including radiative transfer in the Earth's atmosphere [1] and astrophysical media [2,3]. Particularly, an extensive literature concerning the confinement and guidance of radiation in media with radially varying refractive index, usually called GRIN media, does exist. Research on these topics has allowed the design and manufacture of all kinds of devices that involve non-homogeneous media: integrated optics, lenses, waveguides, optical fibers, and diffraction gratings [4,5].

On the one hand, the confinement of radiation in non-homogeneous media with a given refractive index profile has been a highly researched topic. We ourselves, in two previous articles, [6,7], PI and PII hereafter, have analyzed the captured radiation in systems where the refractive index, n, varies smoothly with r, the radial coordinate. Dealing with spherically symmetric systems in PI and with cylindrical symmetry systems in PII, we apply the Fermat's extremal principle in the framework of the geometrical optics to analyze the confinement of the guided radiation in a given region. Analytical solutions of the ray-tracing problem can be found in [8-10]. Also, Evans [11], by comparing the Newtonian mechanics with the laws defining geometrical optics, has calculated the three-dimensional trajectory of a ray propagating through a medium with a parabolic refractive index.

On the other hand, the reconstruction of the unknown refractive index profile of a waveguide according to the behavior that the radiation traveling through it shows is also a highly researched topic: from the first works using interferometric techniques [12] through those based on the measurement of the evanescent field on the surface of the waveguide combined with the use of sophisticated algorithms ([13] and references therein), to one of the newest proposing a non-destructive iterative interferometric tomographic technique [14].

At the present paper, we intend to analyze the confinement of radiation in waveguides useful in both directions: i) given the refractive index profile in the guide, to infer how

the radiation will be guided according to the distance and the angle respect to the axis of the guide with which the radiation entered, and ii) knowing how the radiation travels along with the guide, to obtain information on the radial variation of the refractive index within it and how the radiation entered the guide.

Using the simple criterion we have established in PII that allows us to infer whether radiation confinement occurs in a given system, we intend to contribute to the design of waveguides for predefined objectives, emphasizing on the design of multi-mode guides. Multi-mode waveguides are built with either graded index or step-index. Graded index guides minimize modal dispersion, although they have the disadvantage of being more expensive and difficult to build than step-index guides. In this work, we will address both options.

We organize this paper as follows: In Sec. 2, we set out the basis of our work methodology. In Sec. 3, we analyze the confinement regions of radiation traveling through a waveguide in which i) n takes a constant value a little greater than 1, sharply dropping at the edge (Sec. 3.1) n has a series of steps (Sec. 3.2 and 3.3) n has a parabolic radial variation (Sec. 3.3). In Sec. 4, we address the inverse process, namely, to find the right refractive index profile of the waveguide to radiation travels confined in a given region. In Sec. 5, we present our conclusions.

2. Framework

In PII. we considered a homogeneous transparent cylinder of radius R and infinite length characterized by a refractive index $n > 1$. There, we considered a light ray propagating within the cylinder in an arbitrary direction, but no parallel to the cylinder axis, so that it eventually would strike the cylinder wall in which it would be reflected and refracted. The reflected light would continue traveling inside the cylinder until it again strikes the cylinder wall. If total internal reflection occurs, the process will be repeated over and over again. In Fig. 1 of that paper, that we reproduce here as Fig. 1 for simplicity, we showed the portion between P_1 and P_2 of that endless journey within the cylinder, being P_1 and P_2 the points in the cylinder wall where two successive reflections occur. We defined a Cartesian coordinate system so that the Z-axis is along the cylinder axis, the ray is on a plane which is parallel to the Y-Z plane, and the X-Y plane intersects the ray at P_0, the point which is equidistant from P_1 and P_2.

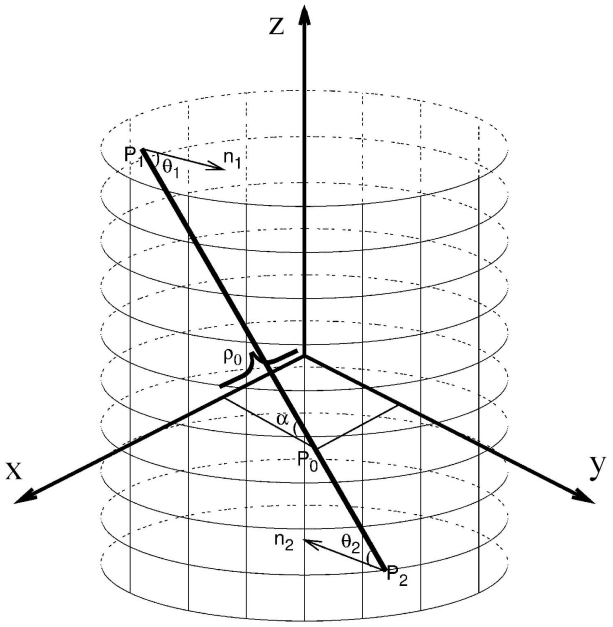

FIGURE 1. Used coordinate system. Coordinate system defined to describe the path of a ray of light in a system with cylindrical symmetry (see text for definition of the parameters).

Considering a system whose refractive index presents a monotonic variation with ρ, the distance from the cylinder axis, and getting rid of the n dependence on ν, the light frequency, we have defined in PII two parameters that fully characterize a given ray: i) $\boldsymbol{\rho_0}$, the distance of closest approach to the Z-axis (the X coordinate of P_0) and ii) α, the angle between the ray and a line parallel to the Y-axis passing through P_0 (see Fig. 1).

In PII, applying the Fermat's extremal principle in the framework of the geometrical optics, we have shown that, in systems with cylindrical symmetry where the refractive index varies smoothly with the distance to the cylinder axis, confinement of radiation does occur, provided it is verified

$$\rho^2 n^2(\rho) = \left[n^2(\boldsymbol{\rho_0}) \sin^2 \alpha\right] \rho^2 + \left[\boldsymbol{\rho_0^2} n^2(\boldsymbol{\rho_0}) \cos^2 \alpha\right]. \quad (1)$$

This expression allows finding a two-dimensional domain defined by the parameters $\boldsymbol{\rho_0}$ and α, that we have called "the confinement region", whose shape is directly related with the function $n(\rho)$.

For a given $n(\rho)$, the confinement region is a region in the ($\boldsymbol{\rho_0}$,α) plane limited by two or more curves. This implies that every pair of values ($\boldsymbol{\rho_0}$,α) within this region represents a possible way in which the rays might enter the waveguide through one of its ends so that they reach the opposite end after traveling along with it. In PII, we have found the curves limiting that region by looking for the solutions of Eq. (1) for each $n(\rho)$ taken as an example.

Now, we will take into account that the limiting curves of the confinement regions could be found by analyzing the Legendre transform of the function defined by the left hand of Eq. (1).

To comprise this, let us consider as an example $n(\rho)$ given by the parabola $n(\rho) = n_0\left(1 - (A\rho^2/2)\right)$ for $\rho < 1$, being n_0 a constant a little higher than unity and A a parameter which is obtained taking into account that $n(\rho) = n_0$ along the cylinder axis ($\rho = 0$) and $n(\rho) = 1$ at the cylinder wall ($\rho = 1$), and let us draw the left hand of Eq. (1) as a function of ρ^2. On the one hand, for the adopted $n(\rho)$, $\rho^2 n^2(\rho)$ is a curve which increases monotonically with ρ^2 until reaching a maximum, softly decreasing afterward to a relative minimum reached at $\rho^2 = 1$, as represented in Fig. 2.

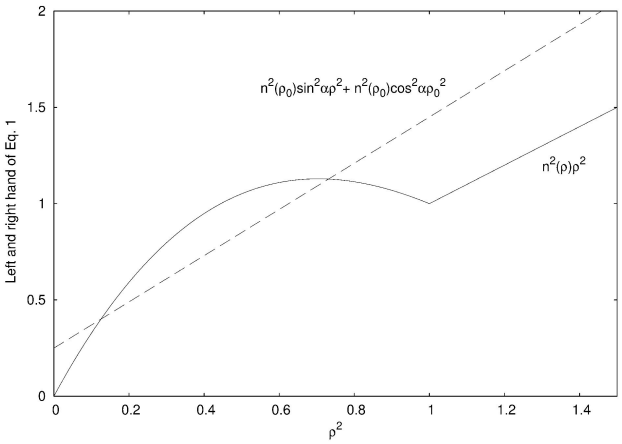

FIGURE 2. Left and right hand of Eq. (1). The left and right hand of Eq. (1) are shown as functions of ρ^2 for given ρ_0 and α values.

Although the maximum of the curve will not occur within the waveguide for n_0 values lower than 1.5, a confinement region will exist, and the analysis we are going to do is quite the same. On the other hand, the right hand of Eq. (1) is always a straight line whose slope and intercept depend on the $\boldsymbol{\rho_0}$ and α values. One of these straight lines, for particular $\boldsymbol{\rho_0}$ and α values ($\boldsymbol{\rho_0} = \mathbf{0.88}$ and $\alpha = 65.5°$), is represented in Fig. 2. Solutions of Eq. (1) are given by the pairs ($\boldsymbol{\rho_0}$,α) for which the functions given by left and right hands of Eq. (1) cut each other twice. It is easy to see that every straight line with slope and intercept values between those corresponding to the tangent lines to the curve represented in Fig. 2 cuts this curve twice. Then, from the equations of these tangent lines, we could get the limiting curves of the confinement regions in the $\boldsymbol{\rho_0}$ and α plane. That family of tangent lines is nothing but a Legendre transform of the function defined by the left hand of Eq. (1).

If $n(\rho)$, rather than being represented by a smooth curve, exhibits a step on the edge of the guide, the curve displayed in Fig. 2 will increase monotonically with ρ^2 until it reaches a maximum at $\rho^2 = 1$ where it will abruptly go down. In this last case, at the same conclusions, we will arrive through a similar analysis.

Using the Legendre transform of the function $y(x)$, instead of the function itself, to find the confinement regions gives us several advantages:

a) it allows us to make a general analysis, applicable in any case regardless of the particular form of $n(\rho)$,

b) it gives us a new space of analysis easier to interpret and visualize, very convenient in the context of our task and

c) let us conclude straightforward manner about the characteristics that our waveguide should have so that the radiation is confined in one or another region according to our interests.

The equivalence of the analysis methods will be verified in the next sections by recovering the results we have reached in PII for the two $n(\rho)$ functions we took as examples at that occasion, namely, one step and parabolic index. At that opportunity, we intended to find the confinement region for a given $n(\rho)$. In the present paper, we also focus on developing the reciprocal process: to find the $n(\rho)$ with which the waveguide should be built for a sought-after confinement region.

3. Looking for confinement regions for a given $n(\rho)$ by using Legendre transform

The function whose Legendre transform we have to find is

$$y(x) = n^2(\rho)x, \tag{2}$$

where $x = \rho^2$.

We intend to pass from the (x, y) to the (u, v) plane through the Legendre transform, doing

$$u = \frac{dy}{dx}, \tag{3}$$

$$v = y[x(u)] - ux(u), \tag{4}$$

where u and v represent the slopes and intercepts of the tangent lines to $y(x)$.

Before continuing, we want to highlight two things. First, regardless of whether $n(\rho)$ is a continuous and derivable function for any ρ value or not, we can always move from the (x, y) to the (u, v) plane by the appropriate considerations. The considerations we are going to do in the following sections to find the equations of the tangent straight lines to $y(x)$ must be interpreted as a way of extending the concept of Legendre transform at the discontinuities. We must keep in mind that the discontinuities, in the context of a physical model of a continuous medium, represent only a very convenient mathematical simplifier alternative for the model. They do not imply, however, essential physical facts.

Second, regardless of the functional form of $n(\rho)$, the slopes and intercepts of all straight lines that cut twice the curve representing $y(x)$ are positive numbers, since all these lines are represented by the right hand of Eq. (1). This restricts the solutions to the first quadrant of the (u, v) plane.

4. Applications of the method

In this section, we aim to apply the methodology exposed in the previous section to particular cases. For the sake of looking for confinement regions by using Legendre transform, we will carry out the analysis for three different $n(\rho)$, two of which were already analyzed in PII, namely: i) $n(\rho)$ takes a constant value a little greater than 1 inside the waveguide and sharply drops to 1 at the edge of it, ii) $n(\rho)$ has a series of steps inside the guide, characterized by a value of $n(\rho)$, n_i, each of them and iii) $n(\rho)$ is a parabola.

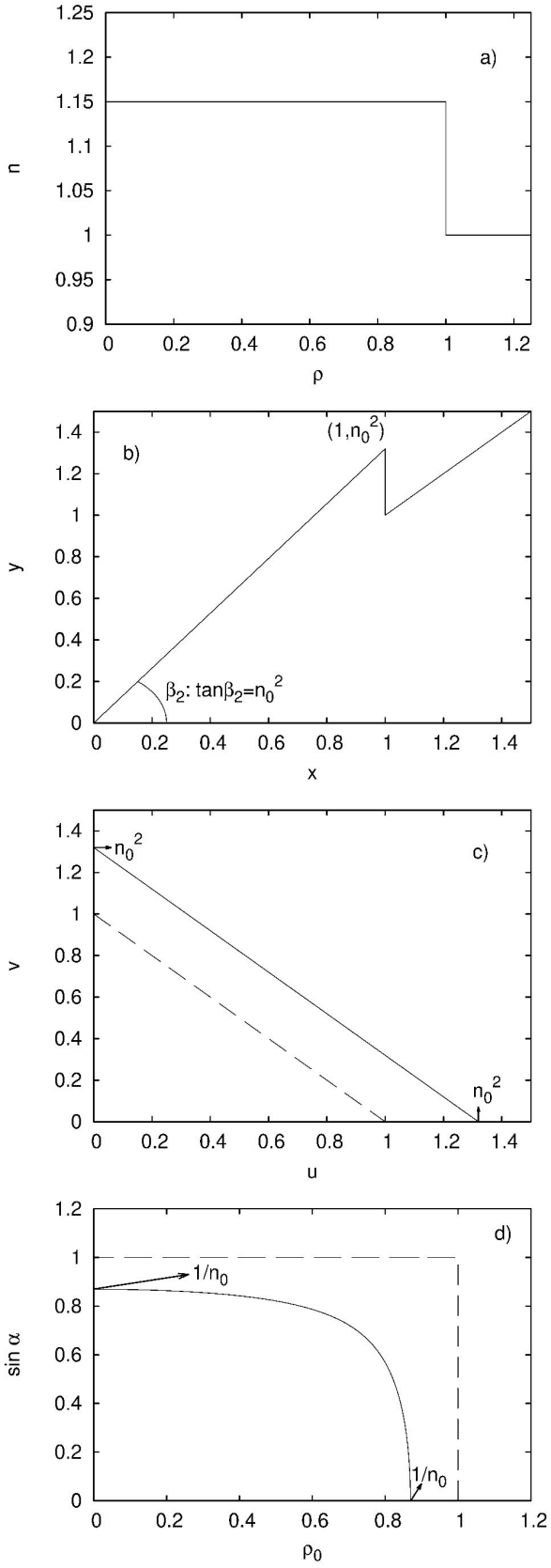

FIGURE 3. One step refractive index profile. For a system characterized by one step refractive, index we display: n as a function of ρ_0 in panel a), y as a function of x in panel b), v as a function of u in panel c), and $\sin\alpha$ as a function of ρ_0 in panel d).

4.1. One step index waveguide

Firstly, let us consider the simplest case: a homogeneous transparent cylinder of radius R and infinite length, which is characterized by a refractive index $\mathbf{n} = n_0 > 1$ relative to the surrounding medium, as displayed in Fig. 3a).

Since $n(\rho) = n_0$ if $\rho < R$ and $n(\rho) = 1$ if $\rho > R$, inside the guide Eq. 2 can be written as

$$y(x) = n_0^2 x. \tag{5}$$

We intend to find, first, the curves in the (u, v) plane that limits the zone of possible slope and intercept values of straight lines that cut $y(x)$ twice.

Even though in the case we are considering $y(x)$ is not a continuous function at $x = 1$, it is easy to get the results we are looking for by making the appropriate considerations.

Firstly, from Fig. 3b) it is easy to see at once that any line cutting $y(x)$ fulfill $u < n_0^2$. Secondly, to cut $y(x)$ twice, the ordinate of any line must be higher than 1 and lower than n_0^2 at $x = 1$.

By taking into account these considerations, it is straight forth to find that all the straight lines that cut the curve drawing in Fig. 3b) twice have a slope and intercept values in a region delimited by the two straight lines

$$v = -u + n_0^2, \tag{6}$$

and

$$v = -u + 1, \tag{7}$$

being Eq. (6) the equation linking slopes and intercepts of every straight line passing through the point $(1, n_0^2)$ and Eq. (7) the equation linking slopes and intercepts of every straight line passing through the point $(1, 1)$. The region in the (u, v) plane limited by Eqs. (6) and (7) is shown in Fig. 3c).

Taking into account that, in order Eq. (1) is satisfied, it must be fulfilled:

$$u = n^2(\boldsymbol{\rho_0}) \sin^2\alpha, \tag{8}$$

and

$$v = \boldsymbol{\rho_0}^2 n^2(\boldsymbol{\rho_0}) \cos^2\alpha. \tag{9}$$

we finally obtain the limits of the confinement region in the plane $(\boldsymbol{\rho_0}, \sin\alpha)$ as

$$\sin^2\alpha = \frac{1 - \boldsymbol{\rho_0}^2 n_0^2}{n_0^2(1 - \boldsymbol{\rho_0}^2)}, \tag{10}$$

$$\sin^2\alpha = 1, \tag{11}$$

$$\boldsymbol{\rho_0} = 1. \tag{12}$$

This region is shown in Fig. 3d), where it is clear that varying n_0 results in a variation of the size of the confinement region: the greater n_0, the greater the confinement region. If the system, instead of being in the air, is a traditional

waveguide consisting of a core with $n = n_0$ and a cladding characterized by $n = n_1$, with $1 < n_1 < n_0$, n_0 should be replaced by n_0/n_1 in Eq. (10).

In PII, the results for a system characterized by a one-step refractive index were given in terms of x and z, being x the X coordinate of any point between P_1 and P_2 on the ray traveling inside the cylinder (since the ray is on a plane which is parallel to the Y-Z plane), and z the Z coordinate of P_2. To show that the expression in PII, reproduced below for simplicity,

$$z^2 = \frac{n^2}{R^2\ (n^2-1)}\left(x^2 - \frac{R^2}{n^2}\right)\left(x^2 - R^2\right)$$

is equivalent to Eq. (10) in this paper, let us make the following considerations. Firstly, since $\boldsymbol{\rho} = \sqrt{x^2+y^2}$ and x is a constant, the shortest distance from the ray to the Z-axis, $\boldsymbol{\rho_0}$, is verified for $y = 0$, which implies that $x = \boldsymbol{\rho_0}$. Secondly, making geometrical considerations, it is found that $z = \tan\alpha\sqrt{1-\boldsymbol{\rho_0}^2}$. Taking into account, finally, that we have adopted $R = 1$ and $n = n_0$, the expression in PII in terms of x and z becomes Eq. (10) of this paper in terms of α and $\boldsymbol{\rho_0}$.

4.2. Multi-step index waveguide

An extension of the previous case is the case for which $n(\rho)$ presents, within the waveguide, a series of steps, rather than a single one. This is the case of multilayer cylindrical waveguide, of great interest for its possible technological applications. Guided radiation achieved by total internal reflection through multilayer waveguides has been analyzed in articles as [15]. Some others, like [16], analyze the multilayer cylindrical waveguide structures by identifying the modal field excitations supported by the corresponding waveguide, regardless of the guiding mechanism.

The case we are considering is the simplest one: $n(\rho)$ within the waveguide is represented by an N steps stair, with equal height and wide all of them, as it is illustrated in Fig. 4a) for $N = 5$. The guide of our example, thus, consists of five regions, R_i, extended from ρ_{i-1} to ρ_i, within each of which $n(\rho) = n_i$, with $i = 1, ...5$. The corresponding $y(x)$, a sawtooth function, is displayed in Fig. 4b).

Although $y(x)$ exhibits discontinuities at every ρ_i, in a similar way to the one used in the previous case for which $n(\rho)$ within the waveguide has a single step, we will be able to find the zones in the (u, v) plane we are looking for. Then, to find the slope (u) and intercept values (v) of the straight lines cutting a certain tooth of $y(x)$ twice, it should be taken into consideration that the ordinate of any such line must be higher than $n_i^2\rho_i^2$ and lower than $n_{i+1}^2\rho_i^2$ at $x = \rho_i^2$, and higher than $n_i^2\rho_{i-1}^2$ at $x = \rho_{i-1}^2$, where i refers to the ith tooth. By taking into account these considerations, it is straight forth to find the equations of the three straight lines that delimit the space of solutions in the (u, v) plane for each tooth, namely:

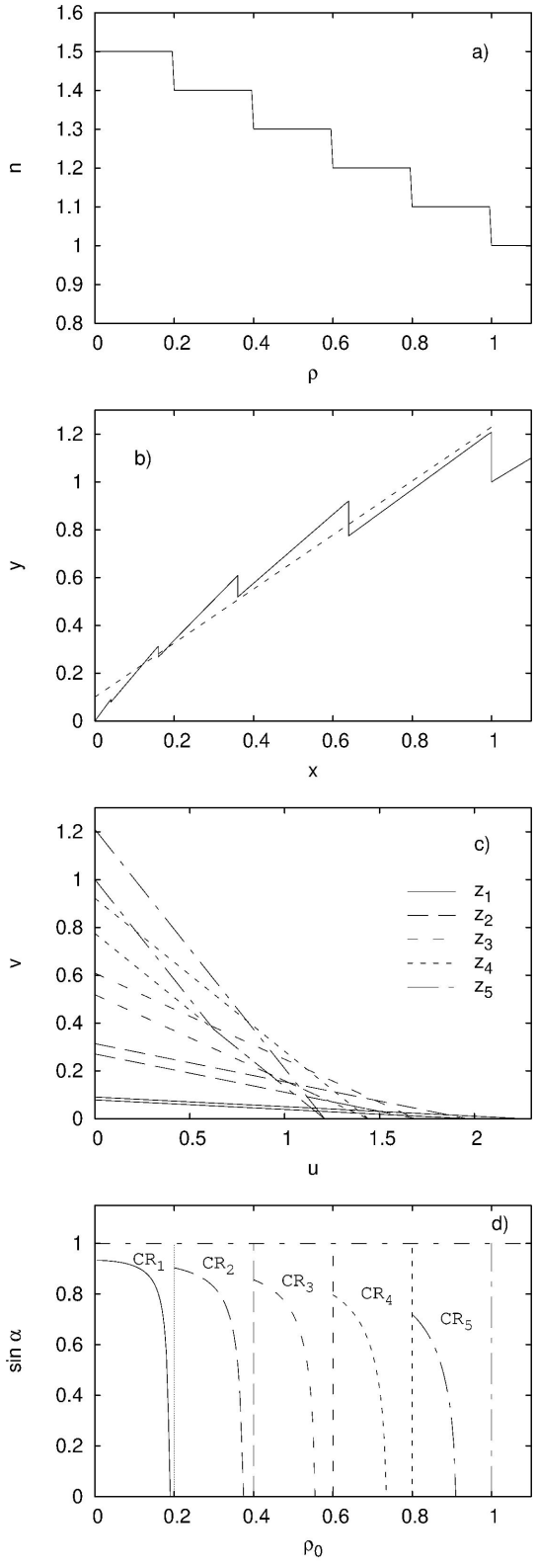

FIGURE 4. Multi-step refractive index profile. For a system characterized by multi-step refractive, index we display: n as a function of ρ_0 in panel a), y as a function of x in panel b), v as a function of u in panel c), and $\sin\alpha$ as a function of ρ_0 in panel d). In panel b), a straight line with slope u_1 and intercept v_1 is also shown (see text).

$$v = -u\rho_i^2 + n_{i+1}^2\rho_i^2, \tag{13}$$

$$v = -u\rho_i^2 + n_i^2\rho_i^2, \tag{14}$$

$$v = -u\rho_i^2 + n_i^2\rho_{i-1}^2. \tag{15}$$

From Eqs. (13), (14) and (15), and taking into account Eqs. (8) and (9), the corresponding confinement regions in the $(\boldsymbol{\rho_0}, \sin\alpha)$ plane are found as limited by

$$\sin^2\alpha = \frac{\rho_i^2 n_{i+1}^2 - \boldsymbol{\rho_0}^2 n_i^2}{n_i^2(\rho_i^2 - \boldsymbol{\rho_0}^2)}, \tag{16}$$

$$\sin^2\alpha = 1, \tag{17}$$

$$\boldsymbol{\rho_0} = \rho_{i-1}, \tag{18}$$

$$\boldsymbol{\rho_0} = \rho_i. \tag{19}$$

Each of the five zones in the (u, v) plane, Z_i hereafter, corresponding to each of the five teeth of $y(x)$, is displayed in Fig. 4c). Therefore, Z_i contains all the possible slope and intercept values of the straight lines that cut the ith tooth twice. Consequently, the different confinement regions in $(\boldsymbol{\rho_0}, \sin\alpha)$ plane, CR_i hereafter, shown in Fig. 4d), contain all possible $\boldsymbol{\rho_0}$ and $\sin\alpha$ values with which the radiation could enter the guide to be confined 'exclusively' in R_i.

However, it is apparent from Fig. 4c) that the spaces of solutions in the (u, v) plane corresponding to the different teeth of $y(x)$ intersect each other. Taking into account expressions (8) and (9) that allow the calculation of $\boldsymbol{\rho_0}$ and $\sin(\alpha)$ for a given $n(\boldsymbol{\rho_0})$ value, it is clear that a given pair of values (u, v) belonging to any of these intersections corresponds to as many different pairs of values $(\boldsymbol{\rho_0}, \sin(\alpha))$ as zones intersected, depending on the corresponding $n(\boldsymbol{\rho_0})$ values. The radiation will be confined in one or another region of the guide depending on the value of $\boldsymbol{\rho_0}$, that is to say, on the distance to the axis with which the radiation enters the guide.

But, even for values of (u, v) belonging to these intersections, radiation will always travel confined exclusively in one, and only one, a region of the guide, R_i.

On the other hand, outside these five zones Z_i, there are (u, v) values for which the radiation remains confined in a sector of the guide, spanning, however, more than one single R_i region. Areas in the (u, v) plane limited by the straight lines given by Eqs. (13) and (14), but not (15), define a strip that differs from the space of solutions for a given tooth in a triangular area like the one labeled $Area\ A$ in Fig. 5b), enlargement of Fig. 4c). Although the $Area\ A$ corresponding to 4th tooth is the only one indicated in the figure, each tooth has its own $Area\ A$. Straight lines with slope and intercept values contained in $Area\ A$ of the ith tooth will cut this tooth where it sharply drops and some other where it ramps upward. This leads to radiation being confined between the two corresponding regions of the guide.

Then, for reasons that will be clearer below, it is important to know how the curves that delimit every confinement region CR_i exhibited in Fig. 4d), defined for $\rho_{i-1} \leq \boldsymbol{\rho_0} \leq \rho_i$ each of them, extend to the $\boldsymbol{\rho_0}$ intervals and the $n(\boldsymbol{\rho_0})$ values corresponding to other regions of the guide, other than R_i. Replacing i with $i-1$ in Eqs. (13), (14) and (15), for example, we find the extension of the curves that delimit the ith confinement region to the interval $\rho_{i-2} \leq \boldsymbol{\rho_0} \leq \rho_{i-1}$, inside which $n = n_{i-1}$, as

$$\sin^2\alpha = \frac{\rho_i^2 n_{i+1}^2 - \boldsymbol{\rho_0}^2 n_{i-1}^2}{n_{i-1}^2(\rho_i^2 - \boldsymbol{\rho_0}^2)}, \tag{20}$$

$$\sin^2\alpha = \frac{\rho_i^2 n_i^2 - \boldsymbol{\rho_0}^2 n_{i-1}^2}{n_i^2(\rho_i^2 - \boldsymbol{\rho_0}^2)}, \tag{21}$$

$$\sin^2\alpha = \frac{\rho_{i-1}^2 n_i^2 - \boldsymbol{\rho_0}^2 n_{i-1}^2}{n_i^2(\rho_{i-1}^2 - \boldsymbol{\rho_0}^2)}. \tag{22}$$

To get curves defined for all $\boldsymbol{\rho_0}$ value lower than ρ_i, similar expressions can be set for each region before R_i. The first and third of these equations extended to the interval $(0, \rho_i)$ are those that limit the region in the $(\boldsymbol{\rho_0}, \sin\alpha)$ plane corresponding to $Area\ A$ of the ith tooth in the (u, v) plane. After that, we will call $Area\ B$ to that region in the $(\boldsymbol{\rho_0}, \sin\alpha)$. In Fig. 6, enlargement of Fig. 4d), $Area\ B$ for 4th tooth is shown.

To make things clearer, let us take as an example the point $(u_1 = 1.13, v_1 = 0.1)$ drawn in $Area\ A$ in Fig. 5b). A straight line with slope $u_1 = 1.13$ and intercept $v_1 = 0.1$ cuts the 4th tooth where it sharply drops and cuts the 3rd tooth where it ramps upward, aside from it cut the 2nd tooth twice, as it is observed in Fig. 5b). Taking into account what we have set in the previous paragraphs, either from Fig. 5b) or Fig. 5c), we should be already able to deduce that it brings to radiation traveling through the 3rd and 4th regions of the guide, R_3 and R_4, respectively, provided that it enters the guide at the suitable distance from its axis $(\boldsymbol{\rho_0})$ and forming with it the suitable angle (α). Otherwise, the radiation might travel confined to R_2.

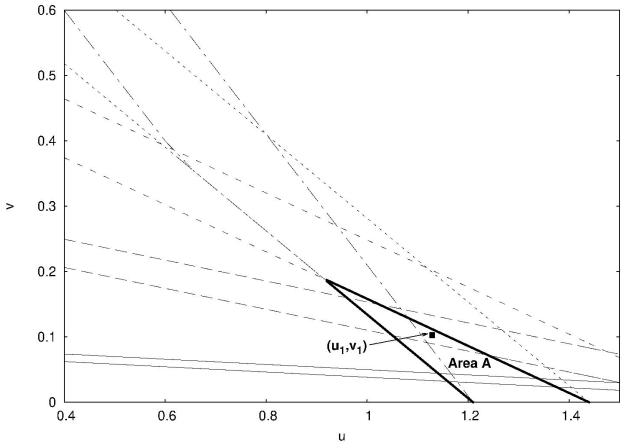

FIGURE 5. $AreaA$ corresponding to the 4th tooth. $AreaA$ corresponding to the 4th tooth (see text for definition) is highlighted in an enlargement of Fig. 4c).

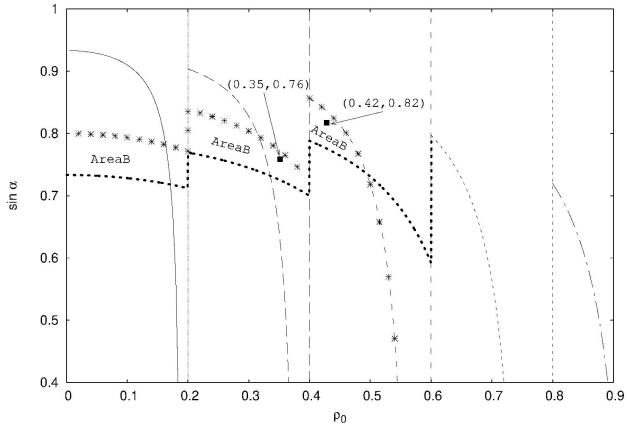

FIGURE 6. $AreaB$ corresponding to the 4th tooth. The $AreaB$ corresponding to the 4th tooth (see text for definition) is included in an enlargement of Fig. 4d).

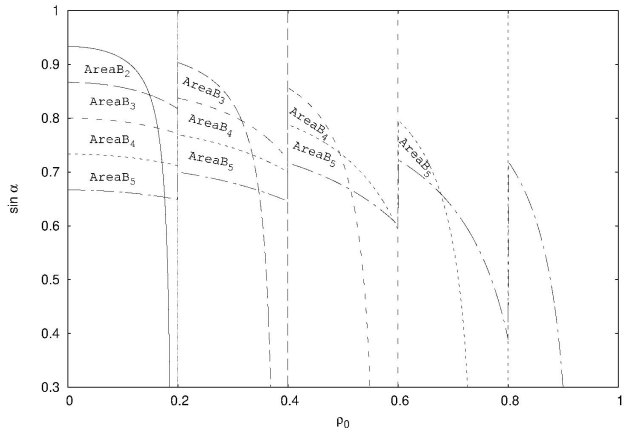

FIGURE 7. $AreaB$ for the five teeth. $\sin\alpha$ as a function of ρ_0 is displayed as in Fig. 4d) but including the curves that delimit the $AreaB$ for the five teeth.

At the same conclusions, we should arrive by analyzing the solutions in the $(\boldsymbol{\rho_0}, \sin(\alpha))$ plane. To find the $(\boldsymbol{\rho_0}, \sin(\alpha))$ values corresponding to (u_1, v_1), and taking into account that u and v depend on $n(\boldsymbol{\rho_0})$, being $\boldsymbol{\rho_0}$ one of the unknowns we intend to find, we should iteratively solve the expressions (8) and (9). The two possible solutions we have found, $(\boldsymbol{\rho_0} = 0.35, \sin(\alpha) = 0.76)$ and $(\boldsymbol{\rho_0} = 0.42, \sin(\alpha) = 0.82)$, are represented by black dots in Fig. 6, both of them located in $Area\ B$, as expected. The meaning of this is as follows: if the radiation enters the guide at a distance of its axis of 0.35 and with an inclination such that $\sin(\alpha) = 0.76$, the radiation will travel through the guide confined in R_2. If, instead, the radiation enters at a distance of 0.42 and with an inclination such that $\sin(\alpha) = 0.82$, the radiation will travel through the guide confined between R_3 and R_4.

For another point (u_1', v_1'), different from the one we have taken as an example but belonging to the same $Area\ A_4$, the radiation might travel between R_4 and some other internal region, R_j, different from R_3. That other region will be the closest to the guide axis, whose defined strip by Eqs. (13) and (14) in the (u, v) plane is located above the point(u_1', v_1'). Although it is immediately deduced from Fig. 4b) or Fig. 4c), it is always possible to analytically find the region R_j, looking for the lowest j value that meets the expression

$$\frac{N^2 v_1'}{j^2} + u_1' < \left[\frac{n_1 N - (n_1 - 1)j}{N}\right]^2, \qquad (23)$$

where $1 \leq j \leq i-1$, N is the number of steps that $n(\rho)$ have within the guide, and n_1 is the value of n in the axis of the guide. The previous expression is valid, provided the steps have all the same height and width. In any case, to any point (u_1', v_1') in (u, v) plane belonging to $Area\ A_4$ corresponds one or more points in the $(\boldsymbol{\rho_0}, \sin(\alpha))$ plane, located all of them in $Area\ B_4$.

Clearly, it is possible to do this for any other point (u_1', v_1') belonging to the $Area\ A$ of some other tooth, different from the 4th.

Finally, for the sake of clarity, a generalization of the results we have achieved in this section is written in the following two paragraphs.

On the one hand, going from (ρ, n) plane to $(\boldsymbol{\rho_0}, \sin(\alpha))$ plane, through (x, y) and (u, v) planes, the following analysis can be done: given a multi-step refractive index profile, any straight line that cuts the ith tooth of the corresponding $y(x)$ where it sharply drops, the jth where it ramps upward, and the hth twice, have a slope, u_1', and intercept, v_1', so that the point (u_1', v_1') is located in the intersection of $Area\ A_i$ and Z_h in the (u, v) plane. It results in two points in the $(\boldsymbol{\rho_0}, \sin(\alpha))$ plane, both of them located in $Area\ B_i$, one of them in the CR_h and the other out of any confinement region CR, and so that $\rho_{j-1} \leq \boldsymbol{\rho_0} \leq \rho_j$. Clearly, this can be generalized to any straight line cutting twice more that one tooth or none at all.

On the other hand, from Fig. 7 where the five $Area\ B_i$ are exhibited along with the five CR_i, we conclude that: i) any pair $(\boldsymbol{\rho_0}, \sin(\alpha))$ located at some CR_i will result in radiation traveling confined in R_i, ii) any pair $(\boldsymbol{\rho_0}, \sin(\alpha))$ located inside some $Area\ B_i$ so that $\rho_{i'-1} \leq \boldsymbol{\rho_0} \leq \rho_{i'}$, but outside of any CR_i, will result in radiation traveling confined between R_i' and R_i, and iii) any pair $(\boldsymbol{\rho_0}, \sin(\alpha))$ located outside of any CR_i and outside of any $Area\ B_i$, will result in radiation no confined at all.

4.3. Parabolic index waveguide

In PII, we have also considered as an example of a system with a parabolic variation of refractive index. Waveguides with n varying this way, first developed by Uchida *et al.* ([17]) and named SELFOC®, is of great interest since it has been shown that a parabolic radial variation of the refractive index considerably decreases distortions and losses. For that reason, it is widely used in optical communication and data processing.

In this case, $n(\rho)$ can be written as

$$n(\rho) = n_0 \left(1 - \frac{A\rho^2}{2}\right), \qquad (24)$$

having n_0 and A the meaning we have set in Sec. 2. For different A values, we have found in PII the confinement regions in the $\boldsymbol{\rho_0}$ and α plane so that Eq. (1) is satisfied.

At the present paper, for $n(\rho)$ given by Eq. (24), we start writing Eq. (2) as

$$y(x) = \left[n_0 \left(1 - \frac{Ax}{2} \right) \right]^2 x, \tag{25}$$

to move from (x, y) plane to (u, v) plane through the Legendre transform.

Then, through Eqs. (3) we obtain

$$u = n_0^2 A \left(\frac{3}{4} A x^2 - 2x + \frac{1}{A} \right), \tag{26}$$

and

$$x = \frac{2}{3A} \left(2 \pm \frac{1}{n_0} \sqrt{n_0^2 + 3u} \right). \tag{27}$$

Replacing Eqs. (27) and (26) in Eq. (4) and taking into account the Eq. (25), we obtain:

$$v = \frac{4}{3A} \left(\frac{\sqrt{n_0^2+3u}}{9n_0} (n_0^2+3u) - \frac{1}{3}(n_0^2+3u) + \frac{4}{9} n_0^2 \right). \tag{28}$$

According to its definition, A can be calculated as

$$A = 2 \left(1 - \frac{n_1}{n_0} \right), \tag{29}$$

where n_1 is the refractive index of the surrounding medium of the system. If the system is in the air, we can set $n_1 = 1$, and Eq. (28) becomes a function of u and the n_0 parameter, which characterizes the system. A, thus, represents a measure of the relative variation of the refractive index on the axis and the edge of the system.

Equation (28) allows us to find one of the limiting curves of the zone in the (u, v) plane containing all slope and intercept values of straight lines cutting $y(x)$ twice. The other can be found taking into account that the ordinate of any straight line cutting $y(x)$ twice must be higher than 1 (n_1^2 if the system is not in the air) at $x = 1$. Then, the other limiting curve is obtained from the expression that slope and intercept of the straight lines passing through the point $(1, 1)$ verify, namely:

$$v = -u + 1. \tag{30}$$

The corresponding confinement region in the $(\boldsymbol{\rho_0}, \sin\alpha)$ plane is obtained by considering that Eqs. (8) and (9) must be fulfilled to Eq. (1) is satisfied.

On the one hand, from Eqs. (8) and (9), and taking into account the expression we have adopted for $n(\rho)$, we obtain:

$$\rho_0^6 - \frac{4}{A}\rho_0^4 + \frac{4}{A^2 n_0^2} \boldsymbol{\rho_0}^2 \left(n_0^2 - u \right) - \frac{4v}{A^2 n_0^2} = 0. \tag{31}$$

The last expression must be solved iteratively for every u value assumed and every v value calculated using expression (28), to obtain the $\boldsymbol{\rho_0}$ value.

Finally, taking into account Eq. (8) the corresponding, α value is calculated as:

$$\sin(\alpha) = \frac{\sqrt{u}}{n(\boldsymbol{\rho_0})}. \tag{32}$$

On the other hand, from Eq. (10), we obtain another curve in the $(\boldsymbol{\rho_0}, \sin\alpha)$ plane that limits the confinement region expressed as

$$\sin(\alpha) = \sqrt{\frac{\frac{1}{n_0^2\left(1-\frac{A\boldsymbol{\rho_0}^2}{2}\right)^2} - \boldsymbol{\rho_0}^2}{1 - \boldsymbol{\rho_0}^2}}. \tag{33}$$

Again, if the system, instead of being in the air, is a traditional waveguide consisting of a core with $n = n_0$ and a cladding characterized by $n = n_1$ so that $1 < n_1 < n_0$, Eqs. (30) and (33) should be replaced by

$$v = -u + n_1^2, \tag{34}$$

and

$$\sin(\alpha) = \sqrt{\frac{\frac{n_1^2}{n_0^2\left(1-\frac{A\boldsymbol{\rho_0}^2}{2}\right)^2} - \boldsymbol{\rho_0}^2}{1 - \boldsymbol{\rho_0}^2}}, \tag{35}$$

respectively.

In Fig. 8, we display four panels. We represent $n(\rho)$, given by Eq. (24), in panel a), $y(x)$, given by Eq. (25), in panel b), the two curves $v(u)$ limiting the zone of solutions, given by Eq. (28) and Eq. (30), in plane c), and the two curves $\sin\alpha(\boldsymbol{\rho_0})$ limiting the confinement region, given by Eq. (32) and Eq. (33), in panel d). In every panel we show the respective functions for two possible n_0 values, $n_0 = 1.15$ and $n_0 = 1.8$. If a system in the air is considered, the corresponding A values, calculated by Eq. (29), turn out to be 0.26 and 0.89, respectively. It is apparent that the set of straight lines, with slope (u) and intercept (v), that could cut twice the curves displayed in Fig. 8b), is larger for higher n_0 values. This means that both, the zone of solutions in the (u, v) plane and the confinement regions in the $(\boldsymbol{\rho_0}, sin\alpha)$ plane, become wider as the value of n_0 increases, as it is clear in Fig. 8c) and Fig. 8d). Then, for a waveguide characterized by a parabolic refractive index, with a very small value of n on its axis (n_0), the radiation may remain confined only if it enters the system forming small angles to its axis.

5. Looking for $n(\rho)$ for a given confinement regions.

In this section, we deal with the reverse problem we have just addressed, namely: given a desired confinement region, to find the right $n(\rho)$. Many aspects of the problem we intend to analyze have been approached experimentally. What we intend in this article is to carry out a theoretical study on the

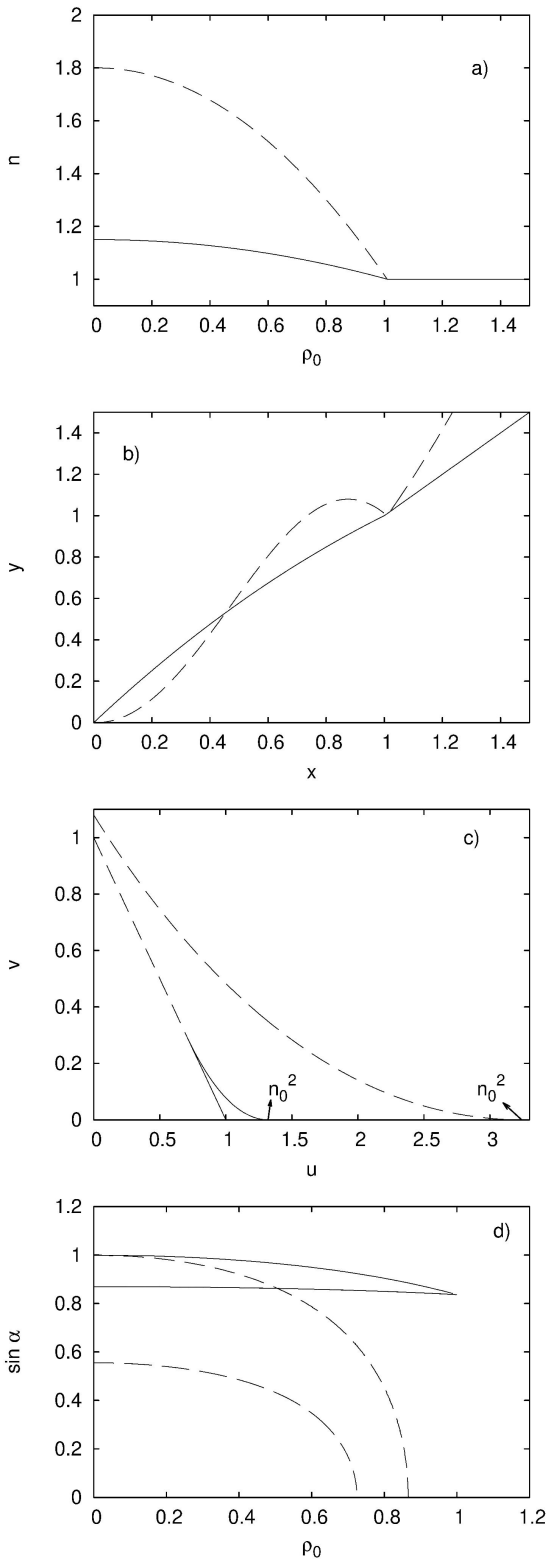

FIGURE 8. Parabolic refractive index profile. For a system characterized by a parabolic refractive, index we display: n as a function of ρ_0 in panel a), y as a function of x in panel b), v as a function of u in panel c), and $\sin\alpha$ as a function of ρ_0 in panel d). Solid lines correspond to $n_0 = 1.15$ and dashed lines correspond to $n_0 = 1.8$, being $n_1 = 1$ in both cases.

topic, reaching analytical or numerical solutions within the framework of the geometric optics we are working with.

For clarity, we will talk in this section in terms of the four planes we have been working with. We call plane a), b), c), and d) (which correspond to panels a), b), c), and d), respectively, in Figs. 3, 4, and 8 to the planes (ρ, n), (x, y), (u, v), and $(\boldsymbol{\rho_0}, \sin\alpha)$, respectively.

In the previous sections, for every $n(\rho)$ taken as an example, we have been able to move from the plane a) to plane d), through planes b) and c), without any complication. For the sake of analyzing the possibility of performing the reverse way, we might think that we could move from plane d) to plane c) because of Eqs. (8) and (9), which link u and v with $\boldsymbol{\rho_0}$ and $\sin\alpha$, are known. Once $v(u)$ is found since we have moved from plane b) to plane c) by means the Legendre transform, we could go the reverse way by means the Legendre inverse transform to find $y(x)$. Then, given $v(u)$, $y(x)$ would be achieved by doing

$$x = -\frac{dv}{du}, \tag{36}$$

and

$$y = v[u(x)] - xu(x). \tag{37}$$

Finally, since $y(x) = n^2(\rho)x$, it could be easy to move from plane b) to plane a) to obtain $n(\rho)$.

Unfortunately, it is not possible to move from $(\boldsymbol{\rho_0}, \sin\alpha)$ to (u, v) if we do not know at all about $n(\rho)$. However, we may arrive at very useful information for our purposes if we know something about the radial behavior of the refractive index within the waveguide.

It is needful to remember that, for one step-index waveguide, for example, u and v are always related by Eq. (6) or Eq. (7) on the curves that limit the zone containing the slope and intercept values of straight lines that cut $y(x)$ twice. In the same way, $\boldsymbol{\rho_0}$ and $\sin\alpha$ are always related by Eqs. (10), (11) or (12) on the borders of the confinement region in the $(\boldsymbol{\rho_0}, \sin\alpha)$ plane. For a multi-step index waveguide, Eqs. (13), (14) or (15) relate u and v on the borders of the spaces of solutions in the (u, v) plane, and Eqs. (16), (17), (18) or (19) relate $\boldsymbol{\rho_0}$ and $\sin\alpha$ on the borders of the confinement regions. Likewise, Eqs. (28) or (30) and Eqs. (32) (along with (31)) or (33) are always verified if the refractive index has a parabolic profile.

What we have expressed in the previous paragraph allows, with some restrictions, to design a waveguide in $(\boldsymbol{\rho_0}, \sin\alpha)$ plane. If the refractive index has a parabolic profile, for example, we can choose $\boldsymbol{\rho_0}$ and $\sin\alpha$ according to the practical needs and then infer the n_0 and A parameters suitable for the case. In other words, the task is to find the range of values that the refractive index could take on the axis of the waveguide and, on the cladding, n_0 and n_1, respectively, so that the radiation entering the system at a distance $\boldsymbol{\rho_0}$ from its axis and forming an angle $90^\circ - \alpha$ with it (recall that α is defined as the angle that the light ray forms with a plane perpendicular to the axis), is guided through the device.

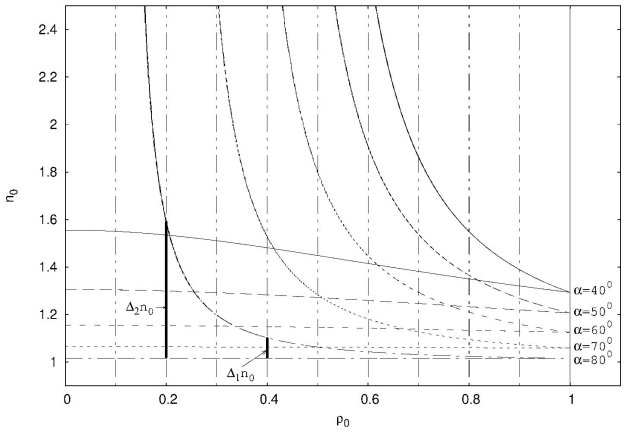

FIGURE 9. n_0 as a function of ρ_0 for different α values. For every α value, two curves are displayed, which enclose the feasible n_0 and ρ_0 combinations so that the radiation is confined.

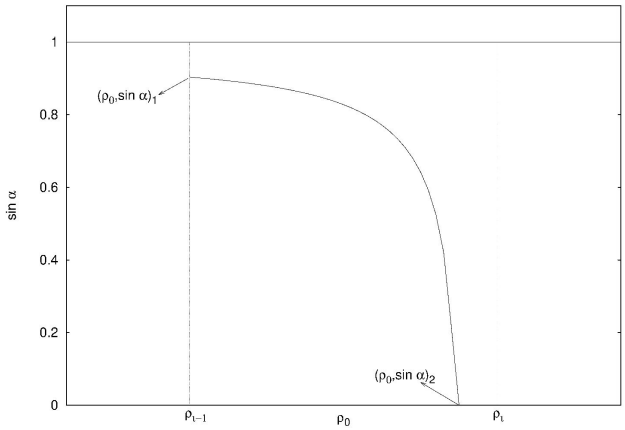

FIGURE 10. Size of the ith confinement region. Curves limiting the ith confinement region in the $(\rho_0, \sin\alpha)$ plane where the parameters defining its size, namely, $(\boldsymbol{\rho_0}, \sin\alpha)_1 = (\rho_{i-1}, \sqrt{[(\rho_i/\rho_{i-1})^2(n_{i+1}/n_i)^2 - 1] \div [(\rho_i/\rho_{i-1})^2 - 1]})$ and $(\boldsymbol{\rho_0}, \sin\alpha)_2 = (\rho_i n_{i+1}/n_i, 0)$, are indicated.

By means Eqs. (28), (30), (31), (32), and (33), which remain valid as long as n have a parabolic radial variation, we have built Fig. 9, where n_0 is represented as a function of $\boldsymbol{\rho_0}$ for different α values. Two curves have been drawn for each of the five α values, from $40°$ to $80°$, we have chosen. The pair of curves corresponding to a given α value limits a region in the $(\boldsymbol{\rho_0}, n_0)$ plane, which contains all possible combinations of n_0 and $\boldsymbol{\rho_0}$ that make the radiation entering the guide with this angle to be confined. In Fig. 9, it is apparent that the two curves corresponding to a given α value tend to the same value of n_0 at $\boldsymbol{\rho_0} = 1$, which can be obtained the by solving the following expression:

$$n_0^3\left[\frac{27}{16}A\left(A-2\right)^2-1\right]+9n_0\sin^2(\alpha)\left(1-\frac{3}{4}A\right) = \left(n_0^2+3\sin^2(\alpha)\right)^{3/2}. \quad (38)$$

The last expression has been obtained from Eqs. (28), (31), and (32) taking into account that $n(\boldsymbol{\rho_0}) = 1$ at $\boldsymbol{\rho_0} = 1$. For n_0 given by Eq. (38), and assuming $n_1 = 1$, the A value at $\boldsymbol{\rho_0} = 1$ can be easily calculated from Eq. (29) for every value of α.

Although Fig. 9 has been built for $n_1 = 1$, it could be done for any n_1 value by solving the corresponding equations iteratively.

From Fig. 9, it follows that, for a given angle with which the radiation enters the guide, the farther from the axis it does, the more precise the n_0 value (for a given n_1) with which the guide should be constructed so that the radiation kept confined. This point is illustrated with two examples included in the figure. Radiation entering the guide making an angle with the axis of $10°$, that is to say, $\alpha = 80°$, at a distance $\boldsymbol{\rho_0} = 0.4$ of it, will remain confined whenever the guide is built with a value of n_0 within the range indicated in the figure as $\Delta_1 n_0$. If, on the other hand, the radiation enters at a distance $\boldsymbol{\rho_0} = 0.2$ from the axis, although with the same angle, the range of values of n_0 with which the guide could be constructed, $\Delta_2 n_0$ in the figure, is greater.

Then, in the figure, a design method consisting in choosing $\boldsymbol{\rho_0}$ and $\sin\alpha$ values and inferring the range of possible values for n_0 y A is proposed. This design criterion takes us directly from plane d) to plane a).

Also, for one-step and multi-step refractive index profiles, clearly, an adequate construction of the guide will allow wider margins in $\boldsymbol{\rho_0}$ and α, facilitating the task of making radiation travel through the regions we want. From what has been analyzed in Sec. 4.1 and 4.2 in the process of finding the confinement regions for theses cases, it is immediate to deduce how the parameters characterizing the system should be varied so that the radiation is confined in one or another region according to the way it enters the waveguide. We only intend to note that, although in (4.2) we have considered $n(\rho)$ represented by five steps, of equal height and wide all of them, from Fig. 4d). The confinement regions are not equal to each other in size.

In Fig. 10, where the confinement region for the ith step is represented, two points, $(\boldsymbol{\rho_0}, \sin\alpha)_1$ and $(\boldsymbol{\rho_0}, \sin\alpha)_2$, are indicated. From the expressions defining the curves that limit this region, it is easy to find the coordinates of these points, which belong to these curves. Indeed, evaluating Eq. (16) at $\boldsymbol{\rho_0} = \rho_{i-1}$, we obtain

$$(\boldsymbol{\rho_0}, \sin\alpha)_1 = \left(\rho_{i-1}, \sqrt{\frac{\left[\left(\rho_i/\rho_{i-1}\right)^2\left(n_{i+1}/n_i\right)^2-1\right]}{\left[\left(\rho_i/\rho_{i-1}\right)^2-1\right]}}\right),$$

and doing $\sin\alpha = 0$ in Eq. (16), we obtain $(\boldsymbol{\rho_0}, \sin\alpha)_2 = (\rho_i n_{i+1}/n_i, 0)$. From these expressions, it is apparent that size and location in the plane $(\boldsymbol{\rho_0}, \sin\alpha)$ of any confinement region can be changed by varying n_{i+1}/n_i and/or ρ_i/ρ_{i-1} ratios.

6. Summary and Conclusions

Based on the criterion we have set in PII applying the Fermat's extremal principle in the framework of the geometrical optics, in this article, we have depicted the radiation confinement regions in the plane $(\boldsymbol{\rho_0}, \sin\alpha)$ for the three refractive index profiles more often used in the construction of waveguides: one step, multi-step and parabolic, respectively. To reach our aim, this time, we have analyzed the feasibility of using the Legendre transform space as an intermediate resource in the process. We have also studied the possibility of performing the reverse path, that is, for a wanted confinement region, to find the parameters characterizing the waveguide to be built. We have analyzed with particular detail the guidance of radiation in multi-step refractive index profile systems. Waveguides characterized by this refractive index profile have numerous technological applications. We conclude, on the one hand, that working in the Legendre transform space to find the confinement regions allows us to reach our goal in any case regardless of the particular form of $n(\rho)$, makes the problem easier to interpret and visualize, and allows us to conclude straightforward manner about the characteristics that our waveguide should have so that radiation is confined in one or another region, according to our interests. On the other hand, we conclude that the reverse path we have referred to is possible as long as we know the power of ρ that defines the radial variation of the refractive index. Then, provided that we know the shape of the profile, our analysis allows us to deduce the characteristics that the guide to be built should have so that the radiation entering with a given angle and at a certain distance from the axis of the guide, remains confined.

If different types of the electromagnetic wave can propagate within the system, the angle and distance from the axis with which the radiation enters the guide, parameters defined according to the technological needs, require to be well differentiated. Choosing those parameters properly, the methodology allows us to define propagation modes through the different regions of the guide, and, in design processes, by building suitably the waveguide, the technique can be used as a resource to limit the parameters that characterize the system.

1. Nener, Brett D.; Fowkes, Neville, and Borredon, Laurent, *J. Opt. Soc. Am. A.*, **20** (2003) 867. https://doi.org/10.1364/JOSAA.20.000867
2. P. M. Kowalski, and D. Saumon, Radiative Transfer in the Refractive Atmospheres of Very Cool White Dwarfs, *ApJ*, **607** (2004) 970. DOI: 10.1086/386280
3. P. M. Kowalski, D. Saumon, and S. Mazevet, Non-Ideal Equation of State, Refraction and Opacities in Very Cool Helium-Rich White Dwarf Atmospheres, *ASP Conference Series*, **334** (2005) 203. Bibcode: 2005ASPC..334..203K
4. D. Marcuser, *Theory of Dielectric Optical Waveguides 2e* (Optics and Photonics Series), 2nd Edition, Academic press Ed. Liao, P. (2012). ISBN: 9780323161770
5. G. P. Agrawal, *Fiber-Optic Communication Systems* (Wiley Series in Microwave and Optical Engineering), 4th Edition (2012). ISBN-10: 0470505117.
6. C. A. Paola, A. Cruzado, P. E. Marchiano, and C. Sorrentino, Capture of electromagnetic radiation in plasmas with diffuse edges. *Optik; International Journal for Light and Electron Optics*, **122** (2011) 1313. https://doi.org/10.1016/j.ijleo.2010.09.009.
7. C.A. Paola, P.E. Marchiano, and A. Cruzado, Confinement of electromagnetic radiation in cylindrical symmetry systems. *Optik; International Journal for Light and Electron Optics*, **125** (2014) 3439. https://doi.org/10.1016/j.ijleo.2014.01.039.
8. E. W. Marchand, Ray Tracing in Cylindrical Gradient-index Media , *Applied Optics*, **11** (1972) 1104. https://doi.org/10.1364/AO.11.001104.
9. E. W. Marchand, Ray Tracing in Gradient-index Media, *JOSA*, **60** (1970) 1. https://doi.org/10.1364/JOSA.60.000001.
10. F. P. Kapron, Geometrical optics of parabolic gradient-index cylindrical lenses , *J. Opt. Soc. Am.* **6011** (1970) 1433. https://doi.org/10.1364/JOSA.60.001433.
11. J. Evans, Simple forms for equations of rays in gradient-index lenses , *Am. J. Phys*., **58** (1990) 773. DOI: 10.1119/1.16357.
12. W. E. Martin, Refractive index profile measurements of diffused optical waveguides. *Applied Optics*, **13** (1974) 2112. https://doi.org/10.1364/AO.13.002112.
13. Wan-Shao Tsai, San-Yu Ting, and Pei-Kuen We, Refractive index profiling of an optical waveguide from the determination of the effective index with measured differential fields, *Optics Express*, **20** (2012) 26766. https://doi.org/10.1364/OE.20.026766.
14. Shengli Fan *et al.*, Optical Fiber Refractive Index Profiling by Iterative Optical Diffraction Tomography, *Journal of Lightwave Technology*, **36** (2018) 5754. DOI: 10.1109/JLT.2018.2876070.
15. Diez, Antonio, Andres, Miguel V., Cylindrical multilayer optical waveguides: applications. *Proceedings of the SPIE*, **2730** (1996) 514. DOI: 10.1117/12.231131.
16. U. Langbein, U. Trutschel, A. Unger, and M. Duguay, Rigorous mode solver for multilayer cylindrical waveguide structures using constraints optimization. *Opt Quant Electron*, **41** (2009) 223. https://doi.org/10.1007/s11082-009-9344-8.
17. T. Uchida, M. Furukawa, I. Kitano, K. Koizumi, and H. Matsumura, Optical Characteristics of a Light-Focusing Fiber Guide and Its Applications, *IEEE J. QE-6*, **10** (1970) 606. DOI: 10.1109/JQE.1970.1076326.